phys. stat. sol. (b) **245**, No. 6, 1125–1132 (2008) / **DOI** 10.1002/pssb.200743364

physica status solidi b
www.pss-b.com
basic solid state physics

# Temperature-dependent Raman scattering of natural and isotopically substituted PbS

**P. G. Etchegoin[*,1], M. Cardona[2], R. Lauck[2], R. J. H. Clark[3], J. Serrano[4], and A. H. Romero[5]**

[1] The MacDiarmid Institute for Advanced Materials and Nanotechnology, School of Chemical and Physical Sciences, Victoria University of Wellington, P.O. Box 600, Wellington, New Zealand
[2] Max-Planck Institut für Festkörperforschung, Heisenbergstraße 1, 70569 Stuttgart, Germany
[3] Christopher Ingold Laboratories, Department of Chemistry, University College London, 20 Gordon Street, London WC1H 0AJ, UK
[4] European Synchrotron Radiation Facility, Boite Postale 220, 38043 Grenoble, France
[5] CINVESTAV-Querétaro, Libramiento Norponiente 2000, Fracc. Real de Juriquilla, 76230 Querétaro, México

Received 6 September 2007, revised 21 November 2007, accepted 10 December 2007
Published online 12 February 2008

**PACS** 63.20.D–, 63.50.–x, 78.30.Am

[*] Corresponding author: e-mail Pablo.Etchegoin@vuw.ac.nz, Phone: +64-04-463 6681, Fax: +64-04-463 5237

Lead sulfide is an important semiconductor that has found technological applications for over a century. Raman spectroscopy, a standard tool for the investigation and characterization of semiconductors, has limited application to this material because of the forbidden nature of its first order scattering and its opacity to visible lasers. Nevertheless, useful vibrational spectra from two-phonon processes are obtained with red lasers, probably because of a resonance in the concomitant electronic transitions. Herewith, we report temperature dependent Raman spectra covering the 10–300 K range, for two samples with different sulfur isotopic compositions. The results are analyzed by comparison with *ab initio* calculations of the lattice dynamics of PbS and the corresponding densities of one and two-phonon states. Emphasis is placed on the analysis of the two phonon band centered at ~430 $cm^{-1}$. The combined use of *ab initio* calculations and an extended temperature range (compared to previous reports) allows an unequivocal identification of some of the main features in the second-order Raman spectra. Our study also provides a much firmer background for the understanding of anomalous temperature dependences in the anharmonic shifts of second-order Raman spectra in PbS.



**1 Introduction** Lead sulfide (PbS), the mineral galena, is an important material in lead smelting [1]. It can be found in nature and also grown as an n- or p-type semiconductor with carrier concentrations as low as $10^{17}$ $cm^{-3}$. Its small electronic gap (0.4 eV), with an anomalous temperature dependence [2], implies small effective masses which make PbS useful as a material for nanostructures [3]. On the negative side, it is a visually offensive black product which appears during the degradation of lead white pigment in artwork [4]. It has been used as a nanoparticle source in very ancient metallic lustre pottery, possibly the oldest known form of controlled nanotechnology [5]. It has also found an age old application in the adulteration of an eye-lining cosmetic called "kohl" ($Sb_2S_3$) [6].

Raman spectroscopy provides a versatile, non-destructive technique for the investigation and characterization of semiconducting materials [7]. The NaCl structure of PbS, however, makes the material first order Raman forbidden. Nevertheless, it has been recently discovered that characteristic Raman spectra are obtained when lasers in the red are used as Raman spectroscopic sources. These spectra are dominated by a band (actually a doublet) centered at around ~430 $cm^{-1}$ and a somewhat narrower peak at ~210 $cm^{-1}$. A few other characteristic weak structures are also observed. These spectra have been recently used for the characterization of lustre pottery and possibly adulterated "kohl" [5, 6].

In a recent publication [8], our group investigated the dependence of the two aforementioned Raman bands on

the isotopic mass of sulfur and on temperature, the latter being limited to the 100–300 K region. The lack of data at lower temperatures hampers the investigation of the mechanisms responsible for the observed anharmonic temperature shifts. Therefore, in the present work we undertook the investigation of these Raman spectra down to a temperature of ~10 K. As in the case of the anomalous temperature dependence of the electronic gap (but most likely unrelated to it) the frequency of the ~430 $cm^{-1}$ band anomalously increases with increasing temperatures, a fact that suggests interaction of each of the two phonons responsible for this ~430 $cm^{-1}$ band with a set of two phonons at lower frequencies (~65 $cm^{-1}$). The dependence of the ~430 $cm^{-1}$ band on the isotopic mass of sulfur, however, is normal and suggests that the corresponding eigenvectors are sulfur dominated (for a general discussion of the dependence of anharmonic self-energies on isotopic masses see Ref. [9]). In order to complete the assignment of the observed Raman structures, we have calculated the phonon dispersion relations of PbS based on an *ab initio* LDA electronic band structure [10]. Using these dispersion relations, which are rather close to the few points measured with inelastic neutron scattering (INS), we have calculated the density of two phonon states for both sums and differences of two phonons, which is relevant to the interpretation of the two-phonon Raman scattering. A thorough discussion of the observed spectra based on the calculated two phonon density of states is given.

**2 Experimental** The samples were similar (in some cases identical) to those used in Ref. [8]. The synthetic samples were grown as discussed in Refs. [8, 11]. The natural PbS samples (95% of $^{32}S$) whose spectra we report were mineral galena (cleaved surfaces) from Creede, Colorado. They were p-type with hole concentrations $N_h \sim 2\times10^{17}$ $cm^{-3}$. The isotopically modified samples were also p-type, with $N_h \sim 10^{18}$ $cm^{-3}$. They were mounted in a closed-cycle He-cryostat (CTI-Cryogenics, Mansfield, MA USA) with temperature control in the range 10–300 K and optical quartz windows. Raman measurements were performed using the 647 nm line of a $Kr^+$-ion laser which was focused to a ~50 μm diameter spot with 50 mW incident power measured at the entrance window of the cryostat. The signal was collected using a photographic zoom lens (Canon, ×10 magnification) of high numerical aperture (0.45) onto the entrance slit of a high-dispersion double-additive U1000 Jobin–Yvon spectrometer coupled to a liquid $N_2$-cooled CCD detector (512 pixels) without any polarization analysis. Integration times in the range 5–15 min (repeated 3 times, for the software to identify and discard spurious cosmic rays in the spectra) were used for different measurements in each window of the spectral range. The high dispersion of the double U1000 spectrometer in the red region (~647 nm) implies that several CCD-windows (eight) are needed to cover the full spectral range from 150 to 550 $cm^{-1}$. Data acquisition of the intrinsically weak second-order spectra is therefore slow and ultimately limited by the long-term stability of the optical system plus cryostat. The chosen integration times were a compromise between signal-to-noise ratio and a total integration time that would allow a full temperature scan within a period of several hours.

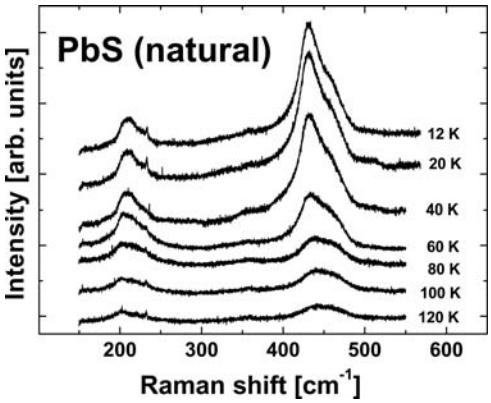


**Figure 1** Raw temperature dependence of the second-order Raman scattering of natural PbS at different temperatures in the range 12–120 K. The data are for 647 nm laser excitation.

Figure 1 shows our raw second-order Raman data for natural PbS at different temperatures. These spectra are dominated by two main features in the ~210 and ~430 $cm^{-1}$ regions. There is evidence in the experimental spectra for substructure in these peaks, to wit: (i) The singularity at ~430 $cm^{-1}$ is clearly a doublet and can be represented as such throughout the entire temperature range by means of two gaussians. (ii) The singularity at ~210 $cm^{-1}$ only reveals itself as a broad doublet at temperatures below ~30 K, as we shall show in what follows. Above ~30 K it is very difficult to isolate its two individual components, most likely because of increasing anharmonic broadening [9].

As already mentioned, the 647 nm $Kr^+$-laser line was one of the few lines with which data could be obtained in both natural and isotopically substituted PbS. Going farther into the visible (in the green, for example, at 514 nm, see Fig. 2 of Ref. [11]) resulted in undesirable (extrinsic) backgrounds that almost completely obliterated the (already very weak) second-order spectra (see also Fig. 8 of Ref. [12]). On the other hand, going into the near-IR region (e.g. the 676 nm line of a $Kr^+$-ion laser) results in very weak intrinsic second-order spectra. Laser excitation around 647 nm seemed to be a good compromise between low background and reasonable signal-to-noise level (possibly aided by a weak resonance effect in the red [11]). Another important experimental detail is the power level of the laser. The surface of PbS tends to be rather sensitive to photodecomposition (mainly, but not exclusively, in the presence of oxygen). The power densities used in these measurements are well below any measurable photodegradation of the surface throughout the total integration time.

The analysis presented here is based on the observation of two main structures in the Raman spectra: (i) one structure at high wavenumbers, around ~430 $cm^{-1}$, which is a doublet and has already been related to the generation of two optical (actually LO) phonons [8, 11] and, (ii) a second structure at ~210 $cm^{-1}$, which is possibly also a doublet but cannot be well resolved in most of the measured spectra and must be related to either two acoustic phonons (2LA) or two optic ones (2TO) as will be discussed later. Our experimental approach is to characterize the behavior of these spectral features as a function of temperature and to ascertain how they differ between natural and isotopically substituted samples. Beside these main features, some weak and broad structures have been surmised at ~160, 340, and 500 $cm^{-1}$. These structures probably correspond to those in Fig. 4 of Ref. [12] at 174, and 320 $cm^{-1}$. In this figure, a rather sharp peak appears at 135 $cm^{-1}$ which is below the frequency range of our spectra and we cannot definitely assign to PbS. The peaks observed in Fig. 4 of Ref. [12] at 600 and 961 $cm^{-1}$ do not seem to correspond to the second-order spectrum of PbS. They are probably due to the $\nu_1$ and $\nu_4$ vibrations of $SO_4^{-2}$ tetrahedra in some form of lead sulfate [13, 14].

Resolving the different peaks which contribute to the main two singularities under discussion is the first step to understand their temperature dependent behavior and, accordingly, their dependence on isotopic mass. The basic limitation here is the lack of a reliable anaytical model for the singularities in the phonon densities of states (see next section) responsible for the second-order scattering observed. Gaussian lineshapes represent the individual singularities rather well, and will be used throughout our analysis. The fact that Gaussian lineshapes work well may also indicate that the shape of the observed structures is heavily influenced by anharmonicity, rather than by the specific type of DOS critical points involved. An additional problem is the reliability of the fits at high temperatures, where even the high energy doublet around ~430 $cm^{-1}$ merges into a visually unresolved single peak, and the signal-to-noise ratio worsens considerably. Fits can still be obtained by restricting the range in which the different parameters are allowed to vary. Resolution of the two components, however, is not a problem at temperatures below ~60 K: at these temperatures the ~430 $cm^{-1}$ peaks are resolved even to the naked eye.

We tried two ways of isolating the different contributions to the singularities as depicted in Fig. 2. One is a direct fit with two Gaussians, an example of which is shown in Fig. 2(a) for the high-wavenumbers feature. An alternative way that works satisfactorily throughout the entire temperature range is also to estimate the energy of the peaks by numerically calculating the second derivatives of the observed spectra (a common practice when dealing with electronic dielectric functions and the related energy gaps); such derivative spectra are shown in Fig. 2(b). In this latter case the analysis becomes independent of the specific lineshape model used to fit the data: the critical

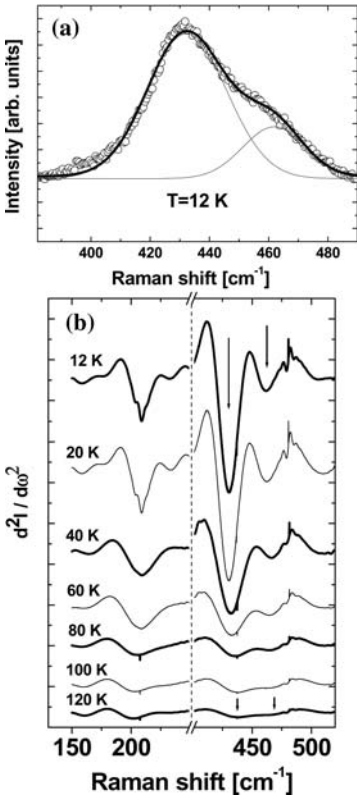


**Figure 2** Analysis of the second-order Raman scattering features of natural PbS. Two approaches have been followed; both giving similar results. In (a) we show the direct fit of the high energy peak with two Gaussians at $T = 12$ K. The fit has a few imperfections in the lineshape but is an acceptable representation of the singularity in the density of states. The *numerical second derivative* approach to the estimation of critical point energies is shown in (b) for both singularities (at high and low wavenumbers) in Fig. 1 (note the break in the horizontal axis). The low wavenumbers "acoustic" feature splits into a clear doublet at low temperatures. The energies of the two peaks in the high energy feature (obtained from the local minimum in $d^2I/d\omega^2$) can be easily followed throughout the entire temperature range. See the text for further details. The arrows show the wavenumbers of the bands contributing to the feature at ~430 $cm^{-1}$ at both $T = 12$ K and 120 K, respectively.

energies can be assigned to the wavenumber of the deepest spectral features in the derivative spectra (see arrows in Fig. 2(b)).

The best comparison between natural PbS and isotopically substituted $Pb^{34}S$ is obtained from the direct observation of the spectra at the lowest achievable temperature in our experimental setup (i.e. 12 K), as shown in Fig. 3. The maximum of the low-wavenumbers feature shifts from ~205 $cm^{-1}$ in natural PbS to ~201 $cm^{-1}$ in $Pb^{34}S$ at 12 K (~2% shift). However, the corresponding lineshapes are not exactly the same and therefore the shift so obtained is not expected to be very precise. The maximum of the high-wavenumbers feature, on the other hand, moves by ~15 $cm^{-1}$, from 432 down to 417 $cm^{-1}$ (3.5%) between the

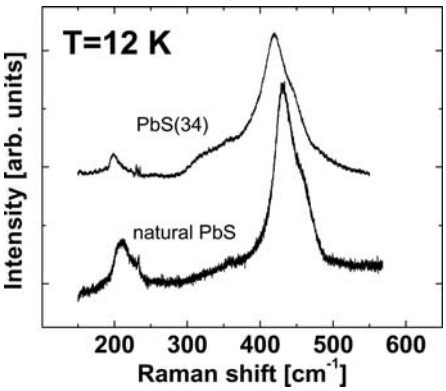


**Figure 3** Comparison of the raw Raman second-order spectra between natural and isotopically substituted $Pb^{34}S$ at 12 K. The shift to lower energies of the singularity at ~430 $cm^{-1}$ can be easily seen with the naked eye. In terms of percentages of change in the energies, the singularity at low wavenumbers (~210 $cm^{-1}$) is less susceptible to a change into a heavier S mass in the isotopically substituted sample.

two samples. Despite differences in the lineshapes between one case and the other, the feature at high wavenumbers seems to be more susceptible to a mass change in S than that at low wavenumbers.

The temperature dependence of the low-wavenumbers feature is difficult to follow for a variety of reasons which include the fact that a doublet cannot be discerned above ~40 K. In addition, this feature does not seem to be very sensitive to the sulfur mass substitution. For a discussion of the dependence of the observed shift with temperature we therefore concentrate on the high-wavenumber feature at ~430 $cm^{-1}$. This feature shifts up in frequency with increasing temperatures (an unusual sign of the shift [9]) Note that the 210 $cm^{-1}$ peak, and that at 150 $cm^{-1}$, both show the usual down-shift with increasing temperatures [8].

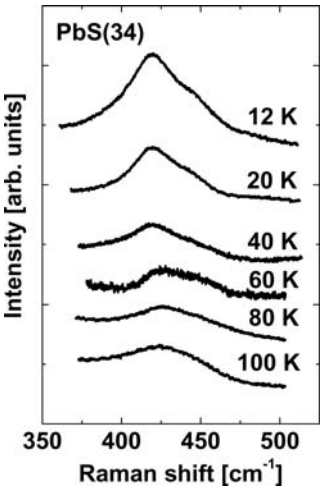


**Figure 4** Temperature dependence of the high-wavenumbers feature in the second-order scattering of $Pb^{34}S$. Both types of analysis of the spectra, i.e. fits with two Gaussians or numerical second-order derivatives cast similar results within ~1 $cm^{-1}$ for the frequencies of the singularities. The temperature dependence of the low-wavenumbers peak in this doublet is displayed in Fig. 5 and compared to the counterpart in natural PbS.

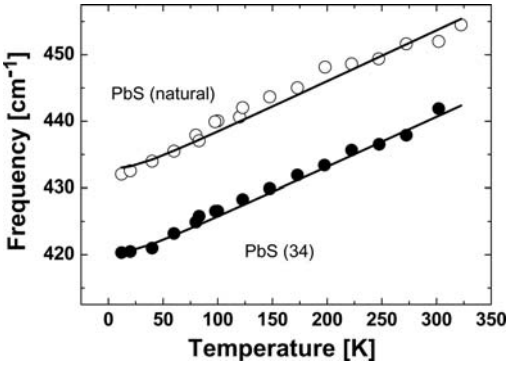


**Figure 5** Temperature dependence of the main peak in the high-wavenumbers feature of the second-order scattering of both natural and isotopically enriched $Pb^{34}S$. The solid lines are fits with Eq. (1). See the text for further details.

Data in the isotopically enriched sample have been taken over a smaller energy range comprising only 3 CCD windows with longer integration times (15 min × 3), in order to obtain the frequency of the peaks with better accuracy. The measurement thus requires 45 min of integration time for each temperature. The temperature dependence of the high-wavenumber feature in $Pb^{34}S$ can be seen in Fig. 4.

Of the two components of this doublet, the one with the highest intensity is the easiest and most reliable to follow as a function of temperature. The second peak, at higher frequencies, becomes very weak above ~40 K and its energy cannot be very accurately determined. We thus concentrate on the temperature dependence of the former which is shown in Fig. 5 for both the natural and the isotopically modified samples.

The data shown in Fig. 5 for both samples exhibit the characteristic temperature dependence expected from anharmonic interactions (the phonon under consideration decaying into two virtual ones). We have used for the fits described below both the data displayed here and those reported in Ref. [8] corresponding to higher temperatures (which overlap only in the ~77–120 K temperature range with our data) [15]. The Raman shift $\omega$ as a function of temperature ($T$) has been fitted with [9]:

$$\omega = \omega_0 + \Delta\omega\left[\frac{2}{e^{T_0/T}-1}+1\right], \qquad (1)$$

where $T_0$ is a characteristic (average) energy (in units of temperature) of each of the two virtual phonons responsible for the main (or average) anharmonic interaction with each of the two "bare" frequencies adding up to the bare $\omega_0$ (i.e. the wavenumber that would be observed if anharmonic effects were not present), $\Delta\omega$ is the *frequency renormalization* at $T = 0$, i.e. the zero-point anharmonic renormalization (the real part of the corresponding self-energy). For $T \to 0$, $\omega \to (\omega_0 + \Delta\omega)$, whilst if $T \gg T_0$,

**Table 1** Parameters of Eq. (1) as fitted to the data in Fig. 5. Typical error bars for these parameters are estimated to be ~0.5 $cm^{-1}$. See the text for further details.

| parameter | PbS (natural) | $Pb^{34}S$ |
|---|---|---|
| $\omega_0$ ($cm^{-1}$) | 428.0 | 415.5 |
| $\Delta\omega$ ($cm^{-1}$) | 5.01 | 4.88 |
| $T_0$ ($cm^{-1}$) | 65 | 65 |

$\omega \propto T$ which is the classical limit [9]. If $4T_0 < \omega_0$ ($\omega_0$ and $T_0$ in the same units) $\Delta\omega$ is positive (because of the sign of the energy denominator in the expression for the real part of the self-energy [9]). Figure 5 shows the best fits to the data with Eq. (1) for both natural PbS and $Pb^{34}S$. The fit parameters are summarized in Table 1. These parameters have, actually, large error bars because the wavenumbers of the peaks change by ~10 $cm^{-1}$ over the full temperature range and are hard to pin down to better than ~1 $cm^{-1}$, as can be easily surmised by visual inspection of the raw data. Based on the information discussed below (*vide infra*) regarding the dispersion relations and the phonon density of states, the following picture of the anharmonic interaction responsible for the temperature shift of the ~430 $cm^{-1}$ mode emerges. The shift is affected by virtual decay into two modes (65 $cm^{-1}$) with basically Pb and very little S character. It is therefore reasonable to fix $T_0$ to be the same for both samples, as was done when performing the fit. This decreases the number of parameters of the combined fits by one and produces more physically meaningful values for the other parameters. Our fits are compatible with a change of ~3% and ~2.4% in $\omega_0$ and $\Delta\omega$, respectively, with the sign of these shifts corresponding to $\omega_0$ and $\Delta\omega$ decreasing with increasing mass, as expected (see next section).

**3 Theory** The interpretation of the phenomenology just described is helped by calculations of the phonon dispersion relations of PbS and the relevant densities of one and two-phonon states (the latter with $\boldsymbol{k}$-vectors equal in magnitude but opposite in sign). Semiempirical calculations are available in the literature [16, 17]; they were performed by fitting a few parameters to a number of experimental frequencies obtained vs. $\boldsymbol{k}$ by inelastic neutron scattering (INS), as reported in Ref. [17]. Here we use parameter-free dispersion relations derived *ab initio* using the ABINIT code [18]. Details of the calculations are given in Ref. [10], which also contains the density of one-phonon states and its projection on the two constituent atoms of PbS. The corresponding densities of two-phonon states with $\boldsymbol{k}_1 = \pm\boldsymbol{k}_2$ (sum as well as difference of the two phonons), were not presented in Ref. [10], and are given here. The "sum" processes are responsible for the anharmonic down-conversion into two phonons of lower energy [19]; while the "difference" anharmonic decay describes the process by which a phonon is destroyed simultaneously with a second low frequency phonon (which must be already in the crystal) and a phonon of higher energy (with respect to the initial one) is created. The difference processes tend to have less importance at low temperatures and vanish for $T \to 0$. Sum and difference processes are not only responsible for anharmonic phonon decay but should also determine the second-order Raman spectra discussed here.

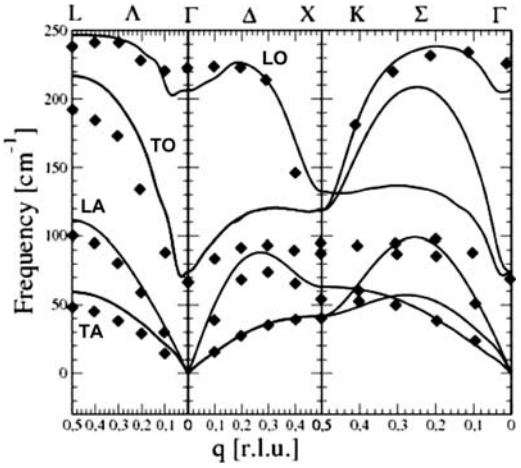


**Figure 6** *Ab initio* phonon band structure calculation of PbS along the principal directions in the Brillouin zone (in reciprocal lattice units: r.l.u.). The points represent experimental determinations from neutron scattering [17]. Note that some of the bands have a much flatter dispersion than that predicted in the model. We shall use experimental points whenever possible and only assign energies to specific bands when the agreement between theory and experiment is good.

Figure 6 shows the *ab initio* calculated dispersion relations of PbS along three principal directions of the Brillouin zone ([100], [111] and [110]). The experimental points obtained with INS are represented by diamonds. The discrepancies which exist between experimental and calculated points are not surprising when one considers that no adjustable parameters have been used in the latter. The largest discrepancies are found for the TO bands. They may be due to anharmonic shifts which affect the experimental data but are not included in the purely harmonic calculations. They are in part included in the semiempirical calculation because of the use of adjustable parameters. One can nevertheless surmise that the *ab initio* calculations should provide an overall better agreement to the *harmonic* dispersion relations than the semiempirical ones. Figures 7 and 8 display the sum and difference DOS obtained through Brillouin zone integration from the dispersion relations of Fig. 6. The results in Figs. 6–8 set the framework for the following discussion.

**4 Comparison with the experiment and discussion** The dispersion relations in Fig. 6 show large regions where the TA bands are rather flat. They give rise to a high and rather narrow peak at ~60 $cm^{-1}$ (see Fig. 2 in Ref. [10]). This peak is likely to correspond to the

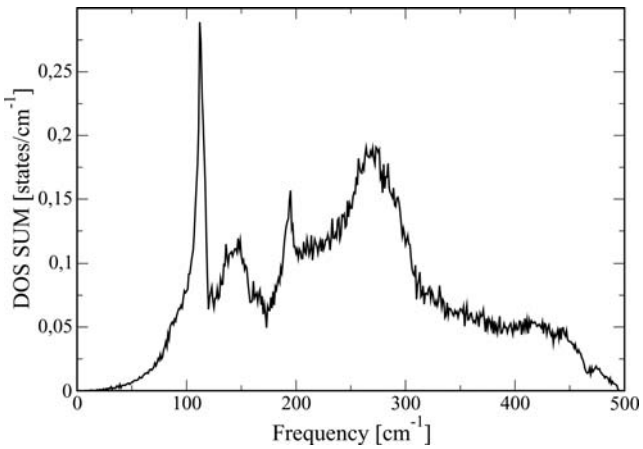


**Figure 7** Phonon sum density of states (DOS) calculated from the dispersion relations in Fig. 6. High wavenumber features related to the LO optical branches have predominantly "S" character, while low wavenumber "acoustic-like" features have mainly "Pb" character. See the text for further details.

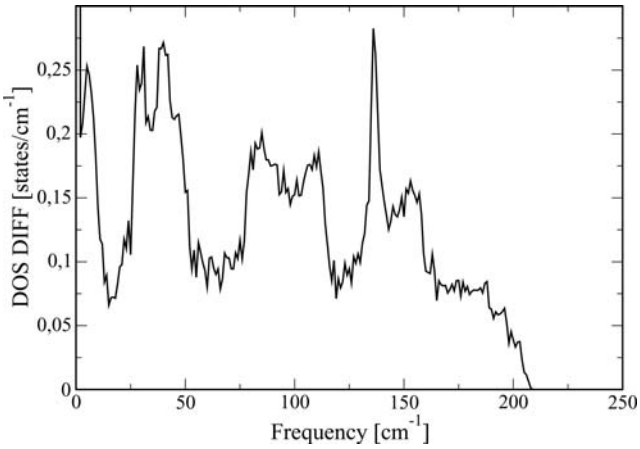


**Figure 8** Two phonon difference density of states (DOS) calculated from the bands in Fig. 6. The difference spectra should occur at the limit of what we can measure at low frequencies in our experimental setup and should also have a distinct temperature dependence disappearing for $T \rightarrow 0$ (which is not observed experimentally on the low energy limit of our observation window). The experimental evidence available at this stage suggests that the observed spectra are dominated by two-phonon sum processes.

frequency $T_0 = 65\ \mathrm{cm}^{-1}$ given in the Table. In Fig. 2 of Ref. [10], the partial contribution of the lead and sulfur vibrations (i.e., the eigenvector components) to the one-phonon DOS is also given. The large mass difference between these two atoms produces a nearly complete frequency separation of the corresponding vibrations: up to ~120 $\mathrm{cm}^{-1}$ the Pb atomic displacements dominate whereas the vibrations above 120 $\mathrm{cm}^{-1}$ are basically dominated by the motion of S atoms. Hence the two phonons contributing to the ~430 $\mathrm{cm}^{-1}$ band should have a squared vibrational amplitude proportional to $(M_S)^{-1/2}$ (where $M_S$ is the atomic mass of the corresponding sulfur isotope). The change of $(M_S)^{-1/2}$ between the two isotopes considered here (natural S is nearly pure $^{32}$S) is 3%, a value which agrees with the fitted variation in $\Delta\omega$ ($\Delta\omega = 2.6\%$).

The densities of states for the sum and difference of two phonons, as obtained from the *ab initio* dispersion relations, are displayed in Figs. 7 and 8. Multiplied by the appropriate Bose–Einstein factors and coupling constants they determine both anharmonic self energies and two phonon Raman scattering intensities. The sharp two-phonon peak seen in Fig. 7 at ~ 120 $\mathrm{cm}^{-1}$ corresponds to the two phonons (each at $T_0 = 60\ \mathrm{cm}^{-1}$) involved in the virtual anharmonic decay of the 430 $\mathrm{cm}^{-1}$ Raman excitations. Several factors need to be considered when comparing second-order Raman spectra with phonon sum or difference DOS. In general, the second-order spectra will resemble (in part) the sum DOS, i.e. only contributions of two phonons, with $+\boldsymbol{k}$ and $-\boldsymbol{k}$ wave vectors, respectively, and either the same (overtones) or different (combinations) frequencies. This is, in fact, how the calculated sum DOS was generated: it contains both overtones and combinations. Although there are many more combinations ($5 \times 6 = 30$) than overtones (6) for each $\boldsymbol{k}$, the overtones seen are often enhanced by the coupling constants (i.e. matrix elements) [20]. A detailed comparison of the Raman spectra with the two-phonon DOS is not justified without the introduction of possibly resonant optical matrix elements and anharmonic self-energies. However, peaks and other structures observed in the two-phonon DOS may find their counterparts in features observed in the Raman spectra. The sets of phonons responsible for the calculated features can be identified by comparison with the dispersion relations. Anharmonic shifts can then be introduced by taking into account the difference between calculated and INS-measured phonon frequencies shown in Fig. 6.

Besides the main ~430 $\mathrm{cm}^{-1}$ band, there is also in the measured spectra the already mentioned ~210 $\mathrm{cm}^{-1}$ band, (note that its frequency decreases with increasing $T$'s [8], i.e. the usual behavior for the shifts of phonons with temperature) and a few other weak bands already reported in Refs. [8, 11, 12].

We make the following tentative assignments of both the main and secondary features:

– The experimental curves have a small (but discernible) feature at about ~160 $\mathrm{cm}^{-1}$. This is at the low energy limit of our experimental range and therefore can only be assigned tentatively. It could correspond to TA + TO (combination band) along $\Sigma$ ($\sim (55+100)\ \mathrm{cm}^{-1} = 155\ \mathrm{cm}^{-1}$). The frequency of this spectral feature also decreases with increasing temperatures [8].

– The experimental peak in the region 205–210 $\mathrm{cm}^{-1}$ seems to have a shoulder at ~230 $\mathrm{cm}^{-1}$ seen clearly at low temperatures. This feature was previously attributed to LO scattering (which is formally forbidden, but can be made allowed and observable by Fröhlich interaction when the laser frequency is near an interband resonance [11]). The data in Refs. [8, 11], which were not taken at low temperatures, did not allow a clear identification of the shoulder at

about ~220 $cm^{-1}$ which could be due to two-phonon scattering. In fact, both features at ~205–210 $cm^{-1}$ could correspond to two-phonon scattering, and it is hard to distinguish this assignment from that to a forbidden LO scattering situation. The sharp peak at ~200 $cm^{-1}$ in the calculated sum DOS corresponds to 2TO phonons either along $\Delta$ or $\Sigma$. One could also take along $\Sigma$ the *experimental* TO + LA values and obtain ~190 $cm^{-1}$. In addition, 2TO at both $\Delta$ and $\Sigma$ should give a feature at ~200 $cm^{-1}$. With suitable weighting by matrix elements, all these assignments may play a role in the Raman feature observed around 210 $cm^{-1}$.

– Combination scattering of LA + LO along $\Sigma$ would give (from the experimental values) ~(100 + 230) $cm^{-1}$ = 330 $cm^{-1}$, or ~340 $cm^{-1}$ along $\Sigma$. This phonon combination could be responsible for the observed experimental weak structure at ~350 $cm^{-1}$.

– The broad peak in the calculated sum DOS centered at ~270 $cm^{-1}$ could be twice the (theoretical) low TO along sigma and have no connection with the experimental phonons (there are no INS points around ~135 $cm^{-1}$ and therefore we do not expect a feature at 270 $cm^{-1}$ in the experiment). The actual TO seems to be lower, possibly because of the anharmonic shift.

– Finally, the asymmetric broad experimental band at ~430 $cm^{-1}$, whose temperature dependence we discussed in the previous section (Fig. 5), could correspond to (using experimental values (INS) for the phonon energies of the bands): (i) 2LO at $\Delta = 2 \times 230\ cm^{-1} = 460\ cm^{-1}$; (ii) 2LO at $\Lambda = 2 \times 245\ cm^{-1} = 490\ cm^{-1}$; and/or (iii) LO + TO at $L$ and $\Lambda = (190 + 240)\ cm^{-1} = 430\ cm^{-1}$.

– For the two-phonon difference DOS in Fig. 8 there is less experimental evidence. Unlike the sum DOS of Fig. 7, the intensity of the features in the difference spectra should vanish at low temperature. Any peak whose intensity vanishes as $T$ approaches the lowest possible temperature (12 K in our case) is a strong candidate to be compared with the difference DOS. We do not see any feature that could safely be assigned to the difference DOS, which exhibits strong structures at 30, 90 and 140 $cm^{-1}$. All these structures lie below the lower limit of the spectral range that can be recorded with our CCD detector without being "swamped" by stray light from the laser. The sharp peak in Fig. 4 of Ref. [12] could be assigned to the peak seen at the same frequency in Fig. 8 (due to LA – TA phonons at $X$ and $\Delta$) if it is confirmed that it belongs to PbS. The best way to buttress this conjecture would be to measure its intensity as the temperature is lowered. Unfortunately, Ref. [12] only reported data obtained at room temperature and our spectrometer does not operate below ~135 $cm^{-1}$.

– Another aspect we have already touched upon concerns the interpretation of the unusual frequency up-shift of the ~430 $cm^{-1}$ feature in Fig. 5 due to virtual anharmonic decay into two phonons. The sign of this coefficient, corresponding to a "blue" shift, is related to the fact that the two-phonon intermediate states are at lower frequency than each of the phonons under consideration ($2 \times 60\ cm^{-1} = 120\ cm^{-1}$ vs. ~215 $cm^{-1}$. The ~215 $cm^{-1}$ modes are all S-like, whereas the 60 $cm^{-1}$ phonons are lead-like. It has been mentioned in the previous section that this leads to a zero-point anharmonic renormalization $\Delta\omega$ proportional to $M_S^{-1/2}$. The corresponding renormalizations for the two isotopes measured are given in the Table. They differ by 2.6%, a value which agrees with that determined from the corresponding isotopic masses of sulfur. For the 205 $cm^{-1}$ peak, regardless of whether it is due only to forbidden one-LO scattering or to two phonon scattering, each with a frequency around 100 $cm^{-1}$, most of the spectral weight of the two phonons with which it interacts lies above the frequency of the phonons being considered (see Fig. 7). There is some experimental evidence for this down-shift in our data (see also Ref. [11]), even though the resolution is poor and the exact nature of the ~210 $cm^{-1}$ peak in terms of one-phonon forbidden scattering or two phonon scattering cannot be unambiguously decided at this stage. Our analysis, however, paves the way for the interpretation of future experimental observations.

– The two components of the ~430 $cm^{-1}$ band must be sulfur like, according to Figs. 6 and 7. Hence they should shift (according to the $M^{-1/2}$ law) by 3% from natural PbS to $Pb^{34}S$. The measured shift, as listed in the Table, is also 3%. We note that we have estimated a somewhat smaller shift (2%) for the measured spectra of the ~210 $cm^{-1}$ band. Although the difference between this shift and that of the square roots of the sulfur masses (3%) lies probably within the experimental error, it would be easy to justify it in terms of the theoretical expectation: For the one-LO scattering the shift should be determined by the reduced mass of Pb and S and amount to 2.6%. In the case of scattering by two phonons, with frequencies around ~100 $cm^{-1}$, which fall in the region which separates Pb-like from S-like vibrations, a shift smaller than that predicted from the sulfur mass can be expected but it is difficult to estimate quantitatively.

**5 Conclusions** We have measured the Raman spectra of two PbS samples, one made out of natural galena and the other a synthetic crystal with natural sulfur replaced by $^{34}S$, in the 150–500 $cm^{-1}$ spectral region at temperatures between 10 and 120 K. These data extend earlier data on the same materials covering the range 100–300 K. For the quantitative interpretation of the spectra we have performed *ab initio* calculations of phonon dispersion relations and the corresponding densities of two-phonon states. The main spectral feature, a broad doublet centered at ~430 $cm^{-1}$, has been assigned to scattering by two LO phonons. Its "anomalous" temperature dependence has been attributed to virtual anharmonic decay into two phonons of frequency ~65 $cm^{-1}$ each. The dependence of the frequencies of the two main observed features on the isotopic mass of sulphur has been shown to agree with theoretical predictions, a fact which we believe buttresses our assignments and interpretation.

**Acknowledgements** P.G.E. acknowledges partial support from the Royal Society of New Zealand (RSNZ) through a Marsden Grant. A.H.R. has been supported by CONACyT México under the project J-42647-F, and by a grant from the University of California, Institute for México and the United States (UC MEXUS), and the Consejo Nacional de Ciencia y Tecnología de México (CoNaCyT). Special thanks are given to Matthias Meyer (Victoria University of Wellington, New Zealand) for the cover image of the paper.

## References

[1] S. Sobanska, N. Ricq, A. Laboudigue, R. Guillermo, C. Bremard, J. Laureyns, J. C. Merlin, and J. P. Wignacourt, Environ. Sci. Technol. **33**, 1334 (1999).
[2] H. J. Lian, A. Yang, M. L. W. Thewalt, R. Lauck, and M. Cardona, Phys. Rev. B **73**, 233202 (2006).
[3] F. W. Wise, Acc. Chem. Res. **33**, 773 (2000).
[4] G. Simkovich and B. Wagner Jr., J. Chem. Phys. **38**, 1368 (1963).
[5] P. Colomban and C. Truong, J. Raman Spectrosc. **35**, 195 (2004).
[6] K. N. Hallad and H. G. Hedderich, J. Hazardous Mater. B **124**, 236 (2005).
[7] P. Y. Yu and M. Cardona, Fundamentals of Semiconductors (Springer Verlag, Berlin, 2001).
[8] R. Sherwin, R. J. H. Clark, R. Lauck, and M. Cardona, Solid State Commun. **134**, 565 (2005).
[9] M. Cardona and M. L. Thewalt, Rev. Mod. Phys. **77**, 1173 (2005).
[10] M. Cardona, R. K. Kremer, R. Lauck, G. Siegle, J. Serrano, and A. H. Romero, cond-mat/0705.1804, submitted to Phys. Rev. B.
[11] G. D. Smith, S. Firth, R. J. H. Clark, and M. Cardona, J. Appl. Phys. **92**, 4375 (2002).
[12] H. Cao, G. Wang, S. Zhang, and X. Zhang, Nanotechnology **17**, 3280 (2006).
[13] G. Herzberg, Molecular Spectra and Molecular Structure (Van Nostrand Reinhold, New York, 1945), p. 167.
[14] L. Burgio and R. J. H. Clark, Spectrochim. Acta A **57**, 1491 (2001).
[15] There is a ~5 $cm^{-1}$ rigid shift in absolute frequencies between the ones determined here and those in Ref. [8]; none of our conclusions depends on this difference (which presumably comes from a calibration difference between the two different spectrometers located in the northern hemisphere and down under) and we have simply shifted the data points from Ref. [8] to get the best possible overlap with the present data.
[16] K. S. Upadhyaya, M. Yadav, and G. K. Upadhyaya, phys. stat. sol. (b) **229**, 1129 (2002).
[17] M. M. Elcombe, Proc. R. Soc. Lond. A **300**, 210 (1967).
[18] X. Gonze, J. M. Beuken, R. Caracas, F. Detraux, M. Fuchs, G. M. Rignanese, L. Sindic, M. Verstraete, G. Zerah, F. Jollet, M. Torrent, A. Roy, M. Mikami, Ph. Ghosez, J. Y. Raty, and D. C. Allan, Comput. Mater. Sci. **25**, 478 (2002).
[19] O. Madelung, Introduction to Solid State Theory (Springer-Verlag, Berlin, 1978).
[20] M. Cardona, in: Light Scattering in Solids II, edited by M. Cardona and G. Güntherodt (Springer Verlag, Berlin, 1982).